CrossMark

ORIGINAL PAPER

Crystal structure and spectroscopic behavior of synthetic novgorodovaite Ca$_2$(C$_2$O$_4$)Cl$_2$·2H$_2$O and its twinned triclinic heptahydrate analog

Oscar E. Piro[1] · **Gustavo A. Echeverría**[1] · **Ana C. González-Baró**[2] · **Enrique J. Baran**[2]

Abstract Synthetic novgorodovaite analog Ca$_2$(C$_2$O$_4$)Cl$_2$·2H$_2$O is identical to its natural counterpart. It crystallizes in the monoclinic $I2/m$ space group with $a = 6.9352(3)$, $b = 7.3800(4)$, $c = 7.4426(3)$ Å, $\beta = 94.303(4)°$, $V = 379.85(3)$ Å^3 and $Z = 2$. The heptahydrate analog, Ca$_2$(C$_2$O$_4$)Cl$_2$·7H$_2$O, crystallizes as triclinic twins in the $P\bar{1}$ space group with $a = 7.3928(8)$, $b = 8.9925(4)$, $c = 10.484(2)$ Å, $\alpha = 84.070(7)$, $\beta = 70.95(1)$, $\gamma = 88.545(7)°$, $V = 655.3(1)$ Å^3 and $Z = 2$. The crystal packing of both calcium oxalate–chloride double salts favors the directional bonding of oxalate, C$_2$O$_4$$^{2-}$, ligands to calcium ions as do other related calcium oxalate minerals. The π-bonding between C and O atoms of the C$_2$O$_4$$^{2-}$ oxalate group leaves sp^2-hydridised orbitals of the oxygen atoms available for bonding to Ca. Thus, the Ca–O bonds in both calcium oxalate–chloride double salts are directed so as to lie in the plane of the oxalate group. This behavior is reinforced by the short O···O distances between the oxygens attached to a given carbon atom, which favors them bonding to a shared Ca atom in bidentate fashion. Strong bonding in the plane of the oxalate anion and wide spacing perpendicular to that plane due to repulsion between oxalate π-electron clouds gives rise to a polymerized structural units which are common to both hydrates, explaining the nearly equal cell constants ~7.4 Å which are defined by the periodicity of Ca-oxalate chains in the framework (monoclinic $b \approx$ triclinic a). When compared with novgorodovaite, the higher water content of Ca$_2$(C$_2$O$_4$)Cl$_2$·7H$_2$O leads to some major differences in their structures and ensuing physical properties. While novgorodovaite has a three-dimensional framework structure, in the higher hydrate, the highly polar water molecules displace chloride ions from the calcium coordination sphere and surround them through OwH···Cl hydrogen bonds. As a result, polymerization in Ca$_2$(C$_2$O$_4$)Cl$_2$·7H$_2$O solid is limited to the formation of two-dimensional Ca$_2$(C$_2$O$_4$)(H$_2$O)$_5$ slabs parallel to (001), inter-layered with hydrated chloride anions. This layered structure accounts for (001) being both a perfect cleavage and a twin interface plane. The infrared and Raman spectra of both salts are also briefly discussed.

Keywords Synthetic novgorodovaite · Heptahydrate analog · Single-crystal X-ray structure · Powder X-ray diffraction · Vibrational spectra

Introduction

Oxalic (ethanedioic) acid is the simplest dicarboxylic acid. The acid and some of its salts have been known since more than 200 years. Its protonation equilibria have often been investigated; the pK values obtained at 25 °C and at ionic strength of 0.1 M are p$K_1 = 1.04$ and p$K_2 = 3.82$ (Martell and Smith 1977), indicating that oxalic acid is a strong organic acid.

The acid generates a great variety of salts and complexes with practically all the known metallic oxides or bases and the oxalate anion is a well-known and widely investigated ligand in coordination chemistry (Cotton et al. 1999). A recent survey of more than 800 oxalate-containing complexes for which structural information is available has

✉ Enrique J. Baran
baran@quimica.unlp.edu.ar

1   Departamento de Física, Facultad de Ciencias Exactas, Universidad Nacional de La Plata and Instituto IFLP (CONICET, CCT-La Plata), 1900 La Plata, Argentina

2   Centro de Química Inorgánica (CEQUINOR, CONICET/UNLP), Facultad de Ciencias Exactas, Universidad Nacional de La Plata, Bvd. 120 N°1465, 1900 La Plata, Argentina

🙋 Springer

shown that the anion possesses 15 different coordination modes with respect to metal centers, and depending on the coordination mode, oxalate ions can form from one to eight metal–oxygen bonds (Serezhkin et al. 2005), confirming the wide versatility of this ligand. It presents four potential binding sites and can act in a mono- or bidentate fashion, forming mononuclear or polynuclear metal complexes.

Metallic crystalline oxalates are also found in different natural environments and in a variety of living organisms, constituting a group of relatively rare minerals usually classified as "organic minerals" (Strunz and Nickel 2001; Echigo and Kimata 2010). Twenty-one of such natural oxalates have so far been identified and characterized (Baran 2016).

Calcium oxalate minerals (the mono-, di- and trihydrates of $[Ca(C_2O_4)]$, are the most common family of organic minerals present in natural environments, usually occurring in carbonate concretions, marine and lake sediments, hydrothermal veins and lignite (Echigo and Kimata 2010). They are also the most common and abundant class of biominerals found in the plant kingdom (Webb 1999; Nakata 2003; Franceschi and Nakata 2005; Baran and Monje 2008; Echigo and Kimata 2010).

Apart from the mentioned hydrated calcium oxalates, a fourth, rarer calcium oxalate, was found in 2001 in the Chelkar salt dome, western Kazakhstan, associated with anhydrite, gypsum, halite, bishofite, magnesite and hilgardite. Its crystallographic structural analysis was consistent with the idealized formula $Ca_2(C_2O_4)Cl_2 \cdot H_2O$ and the name novgorodovaite was proposed for this new mineral (Chukanov et al. 2001; Rastsvetaeva et al. 2001). A synthetic analog as well as a higher hydrate, $Ca_2(C_2O_4)Cl_2 \cdot 7H_2O$, was reported more than half a century ago (Jones and White 1946).

As a continuation of our studies of synthetic analogs of natural oxalates (D'Antonio et al. 2007, 2009, 2010; Mancilla et al. 2009a; Piro et al. 2016), we have prepared the two synthetic chloride-oxalates to establish their possible relations to novgorodovaite.

Materials and methods

Synthesis of the two hydrates

All reagents, of analytical grade, were purchased commercially and used as received. Elemental analysis (C and H) was performed on a Carlo Erba model EA 1108 elemental analyzer.

The heptahydrate was prepared by heating one part of calcium oxalate monohydrate with fifteen parts by weight of 8.6 N hydrochloric acid, in a glass-stoppered flask, until the solid phase completely disappeared. On cooling to room temperature, the heptahydrate crystallized as colorless very thin (less than 0.03 mm thick) and parallelogram-shaped crystal plates. The compound was collected on a fritted glass funnel, washed several times with absolute ethanol and air-dried (Jones and White 1946). The compositional data are as follows: Calculated for $C_2H_{14}Ca_2Cl_2O_{11}$: C, 6.57; H, 3.83. Found: C, 6.50; H, 3.87%.

Multiple attempts to prepare the dihydrate following the methodology proposed by Jones and White (1946) failed, as the obtained samples were always contaminated with different amounts of the heptahydrate. Therefore, we implemented a slightly different experimental procedure as follows: 1.60 g of $CaC_2O_4 \cdot H_2O$ (0.01 mol) was suspended in 16 mL of concentrated hydrochloric acid ($\delta = 1.19$ g mL^{-1}). The mixture was immediately introduced in the glass tube of a hydrothermal bomb and maintained for half an hour at 100 °C. After cooling, a colorless microcrystalline material, constituted by very small prismatic crystals (length dimensions less than 0.13 mm), was collected and treated in the same way as described above. The compositional data are as follows: Calculated for $C_2H_4Ca_2Cl_2O_6$: C, 8.72; H, 1.45. Found: C, 8.66; H, 1.48%.

X-ray crystallographic studies

The X-ray measurements were performed on an Oxford Xcalibur Gemini, Eos CCD diffractometer with graphite-monochromated MoKα ($\lambda = 0.71073$ Å) radiation. X-ray diffraction intensities were collected (ω scans with ϑ and κ-offsets), integrated and scaled with the CrysAlisPro (2014) suite of programs. The unit cell parameters were obtained by least-squares refinement (based on the angular settings for all collected reflections with intensities larger than seven times the standard deviation of measurement errors) using CrysAlisPro. Data were corrected empirically for absorption employing the multi-scan method implemented in CrysAlisPro.

$Ca_2(C_2O_4)Cl_2 \cdot 2H_2O$: the identical unit cell parameters (to within experimental error) and space group symmetry demonstrated that the synthetic dihydrate was the same phase as natural novgorodovaite. An initial model structure based on the non-H atomic parameters reported for natural novgorodovaite (Rastsvetaeva et al. 2001) converged smoothly when refined with SHELXL (Sheldrick 2008) against the data set of the synthetic mineral. The independent hydrogen atom of the water molecule was located in a Fourier difference map based on the heavier atoms and refined at the positions indicated with an isotropic displacement parameter.

$Ca_2(C_2O_4)Cl_2 \cdot 7H_2O$: Most part of the diffraction pattern was interpreted in terms of twin formed by two individuals related to each other through a rotation of 180º around an axis perpendicular to (001) plane. The unit cell parameters

for both individuals were equal to within experimental errors. The reflections were indexed in the reciprocal unit cell of the corresponding components of the twin. It was resorted to the twin crystal data reduction procedure implemented in CrysAlisPro (2014) to generate three data sets, namely a regular one with the diffraction data indexed in the reciprocal unit cell of one domain (hereafter called twin component #1), a second one where overlapping reflections with twin component #2 to a degree higher than 80% were removed from twin #1 data set and a third data set including all the reflections from both domains with the overlapping ones flagged for structure development and refinement.

The full data set for twin component #1 (with about 50% of diffracting power) was employed to solve the structure by the intrinsic phasing procedure implemented in SHELXT (Sheldrick 2008) and the corresponding non-H molecular model refined using isotropic displacement parameters with SHELXL (Sheldrick 2008). Despite a correct molecular model, however, the refinement showed evidence of the presence of strong overlap of reflections from both twin components. This evidence included a relatively high $R1$-value for this stage ($R1 = 0.1482$), spurious large peaks in the residual electron density maps ($\Delta\rho = 5.04$ e Å^{-3}), and the most disagreeable reflections list showing systematically larger F(obs) as compared with F(calc) values. We, therefore, refined the initial molecular model against the second data set, where offending overlapped reflections (affected by an overlap larger than the 80%) were omitted. As expected, the isotropic refinement improved substantially. In fact, in this case the agreement factor dropped to $R1 = 0.0713$, the maximum residual electron density was 1.22 e Å^{-3} and the sign of F(obs)–F(calc) difference for the most disagreeable reflections was more evenly distributed. Further anisotropic refinement followed by a Fourier difference map showed all water hydrogen atoms. These were refined with isotropic displacement parameters at their found positions with Ow–H and H···H distances restrained to target values of 0.86(1) and 1.36(1) Å, respectively. The final R-factor with this partial data set was $R1 = 0.0429$ and the residual electron density $\Delta\rho = 0.43$ e Å^{-3}. There was, however, a cost to be paid. In fact, because of the omission of overlapped reflections, the ratio of the number of observed reflections to the number of refined parameters ratio was rather small (=7.45). Also some water H-atoms showed anomalously large displacement parameters. We then resorted to the third data set, which includes all collected reflections for both crystal domains, and refined the molecular model against these data through the untwining process implemented in SHELXL. Now, the final agreement $R1$-factor was 0.0351, $\Delta\rho = 0.40$ e Å^{-3}, the occupancy of domain #1 was 0.509(1), and the hydrogen displacement parameters converged to acceptable values. Because we are now dealing with the diffraction data from two domains of the same solid, the observed data to parameter ratio increased to 14.91.

Crystal data, data collection procedure, and refinement results for both salts are summarized in Table 1. Crystallographic structural data have been deposited at the Cambridge Crystallographic Data Centre (CCDC). Enquiries for data can be direct to: Cambridge Crystallographic Data Centre, 12 Union Road, Cambridge, UK, CB2 1EZ or (e-mail) deposit@ccdc.cam.ac.uk or (fax) +44 (0) 1223 336033. Any request to the Cambridge Crystallographic Data Centre for this material should quote the full literature citation and the reference number CCDC 1524180 (synthetic novgorodovaite, $Ca_2(C_2O_4)Cl_2\cdot2H_2O$) and CCDC 1524181 ($Ca_2(C_2O_4)Cl_2\cdot7H_2O$).

Powder X-ray diffraction (PXRD)

The PXRD pattern of both salts was obtained with a PANalytical X´Pert PRO diffractometer, using CuKα radiation ($\lambda = 1.5406$ Å) from an X-ray tube operated at 40 kV and 40 mA. The X-ray diffraction patterns were collected in the $2° \leq 2\theta \leq 60°$ range, with 0.02° step width and 1 s counting time per step employing the Bragg–Brentano θ–θ geometry, a scintillation counter, and an exit beam graphite monochromator.

Spectroscopic measurements

The infrared absorption spectra in the frequency range between 4000 and 400 cm^{-1} were recorded on KBr pellets with a FTIR-Bruker-EQUINOX-55 spectrophotometer and using a pure KBr pellet as reference. Raman dispersion spectra were obtained in the 3500–400 cm^{-1} spectral range with a Thermo Scientific DXR Raman microscope, using the 532 nm line of a Thermo Scientific solid-state laser diode pump for excitation (power laser beam = 10 mW).

Results and discussion

Crystal structures

Synthetic novgorodovaite. The crystal structure is shown as an ORTEP plot (Farrugia 1997) in Fig. 1, while selected bond distances and angles are listed in Table 2. All but the oxalate oxygen and water hydrogen atoms are at special crystal positions. In fact, calcium and chloride ions are at *m*-mirror planes, the oxalate carbon atom is on the two-fold axis of a crystallographic C_{2h} site symmetry that renders strictly planar the $C_2O_4^{2-}$ anion, and the water molecule is located on a C_2 two-fold axis.

Table 1 Crystal data and structure refinement results for $Ca_2(C_2O_4)Cl_2\cdot2H_2O$ and $Ca_2(C_2O_4)Cl_2\cdot7H_2O$

	$Ca_2(C_2O_4)Cl_2\cdot2H_2O$	$Ca_2(C_2O_4)Cl_2\cdot7H_2O$
Empirical formula	$C_2H_4Ca_2Cl_2O_6$	$C_2H_{14}Ca_2Cl_2O_{11}$
Formula weight	275.11	365.19
Temperature (K)	297(2)	297(2)
Crystal size (mm³)	$0.127 \times 0.049 \times 0.044$	$0.403 \times 0.328 \times 0.027$
Crystal system	Monoclinic	Triclinic
Space group	$I2/m$	$P\bar{1}$
Lattice parameters		
a (Å)	6.9352(3)	7.3928(8)
b (Å)	7.3800(4)	8.9925(4)
c (Å)	7.4426(3)	10.484(2)
α (°)	90.0	84.070(7)
β (°)	94.303(4)	70.95(1)
γ (°)	90.0	88.545(7)
Volume (Å³)	379.85(3)	655.3(1)
Z	2	2
D_{calc} (g/cm³)	2.405	1.851
Absorption coeff. (mm⁻¹)	2.188	1.320
$F(000)$	276	376
θ-range data collection (°)	3.874–25.997	2.915–28.945
Index ranges	$-6 \le h \le 8$, $-8 \le k \le 8$, $6 \le l \le 9$	$-9 \le h \le 9$, $-12 \le k \le 12$, $-13 \le l \le 13$
Reflections collected	693	4250
Independent reflections	400 [$R(int) = 0.0221$]	5250 [$R(int) = 0.0416$]
Observed reflect. [$I > 2\sigma(I)$]	362	3146
Refinement method	Full-matrix least sq. on F^2	Full-matrix least sq. on F^2
Data/restraints/param.	400/0/36	4250/21/211
Goodness-of-fit on F^2	1.132	0.945
Final R indices[a] [$I > 2\sigma(I)$]	$R1 = 0.0317$, $wR2 = 0.0774$	$R1 = 0.0351$, $wR2 = 0.0794$
R indices (all data)	$R1 = 0.0355$, $wR2 = 0.0823$	$R1 = 0.0544$, $wR2 = 0.0838$
Larg. dif. peak and hole (e Å⁻³)	0.59 and -0.64	0.39 and -0.34

[a] $R1 = \Sigma||F_o| - |F_c||/\Sigma|F_o|$, $wR2 = [\Sigma w(|F_o|^2 - |F_c|^2)^2/\Sigma w(|F_o|^2)^2]^{1/2}$

Fig. 1 Crystal packing projections of synthetic novgorodovaite, $Ca_2(C_2O_4)Cl_2\cdot2H_2O$, showing the labeling of the non-H atoms and their displacement ellipsoids at the 50% probability label; **a** down the *a*-axis; **b** down the *b*-axis. Carbon, oxygen, calcium and chloride atoms are, respectively, shown by *open*, *hatched*, *crossed*, and *grayed* ellipsoids. For clarity, only a few OwH···Cl bonds are shown (by *dashed lines*)
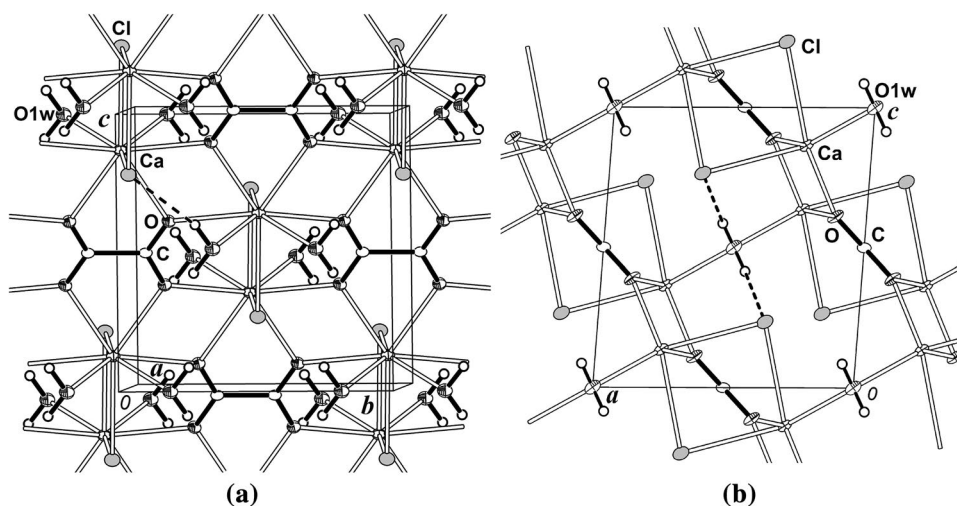
Table 2 Selected bond lengths (Å) and angles (°) for synthetic novgorodovaite mineral, $Ca_2(C_2O_4)Cl_2 \cdot 2H_2O$

Bond lengths (Å)		Angles (°)	
C–O	1.258(2)	O–C–O#1	126.9(3)
C–C#1	1.548(7)	C–O–Ca	117.1(2)
Ca–O	2.432(2)	C–O–Ca#4	132.7(2)
Ca–O#2	2.521(2)	Ca–O–Ca#4	110.20(6)
Ca–O(1W)	2.501(1)	Ca–O(1W)–Ca#5	112.6(1)
Ca–Cl	2.804(1)		
Ca–Cl#3	2.859(1)		

Symmetry transformations used to generate equivalent atoms: (#1) $-x, -y, -z + 1$; (#2) $-x + 1/2, -y + 1/2, -z + 3/2$; (#3) $-x + 1, -y, -z + 2$; (#4) $-x + 1/2, -y + 1/2, -z + 3/2$; (#5) $-x, -y, -z + 2$

The calcium ion is in a distorted eight-fold polyhedral coordination (CaL_8) with an oxalate ion acting as a bidentate ligand [$d(Ca-O) = 2.432(2)$ Å] and with one carboxylate oxygen on each of two neighboring oxalate ions, symmetry-related by a unit-cell b-translation, through the other oxygen electron pair lobe [$d(Ca-O') = 2.521(2)$]. The coordination is completed by two symmetry-related water molecules [$d(Ca-Ow) = 2.501(2)$ Å] that bridge neighboring calcium ions through the water oxygen electron pair lobe and two equivalent chlorine ions [Ca–Cl distances of 2.804(1) and 2.859(1) Å].

The complex three-dimensional crystal packing of the salt favors the directional bonding of oxalate $C_2O_4^{2-}$ ligands to calcium ions through the oxygen sp^2 electron pairs whose lobes lay onto the molecule plane and are oriented at about 120° from each other [observed C–O–Ca angles of 117.1(2) and 132.7(2)°]. This simple MO interpretation of the oxalate bonding is supported by experimental electron density determinations from low-temperature

high-resolution X-ray diffraction of the related oxalic acid dihydrate (Zobel et al. 1992). The arrangement of the solid parallel to the (ac) plane can be viewed as CaL_8 ($CaO_4Ow_2Cl_2$) polyhedra linked through C_2O_4 spacers and Ow···Ow and Cl···Cl shared edges. The crystal packing along the unique b-axis can be described as a zig–zag arrangement of polyhedra where neighboring CaL_8 units are linked to each other through O(ox)···O(ox) sharing edges. This arrangement gives rise to a chain structure along b axis with repeatability equal to the length of this axis [$b = 7.3800(4)$ Å]. Similar chain arrangement of calcium coordination polyhedra where the oxalate ions acts as molecular spacers between neighboring Ca(II) ions though their oxygen electron pairs is also observed in the related $Ca(C_2O_4) \cdot H_2O$ [whewellite, $P2_1/n$ space group; chain along b, where $b = 14.5884(4)$ Å is duplicated (Deganello and Piro 1981)] and $Ca(C_2O_4) \cdot 2H_2O$ [weddellite, $I4/m$; chain along c, $c = 7.357(2)$ Å (Tazzoli and Domeneghetti 1980; Mills and Christy 2006)] minerals. In both cases, the oxalate ions also act as molecular spacers between neighboring Ca(II) ions though their oxygen electron pairs and this is the reason why all three salts present nearly the same cell parameter (about 7.3 Å) along the chain (Rastsvetaeva et al. 2001).

The $Ca_2(C_2O_4)Cl_2 \cdot 2H_2O$ crystal is further stabilized by a OwH···Cl bond [$d(H···Cl) = 2.32(4)$ Å, $\angle(Ow-H···Cl) = 163(3)°$] rather than the weak OwH···O bond with the oxygen atoms of the oxalate anions reported by Rastsvetaeva et al. (2001).

$Ca_2(C_2O_4)Cl_2 \cdot 7H_2O$: Fig. 2 shows the crystal packing of the heptahydrated salt and bond distances and angles are detailed in Table 3. All atoms are at crystal general positions. There are two independent calcium and oxalate ions, with these latter anions on crystallographic inversion centers. Though not constrained by crystal symmetry as in
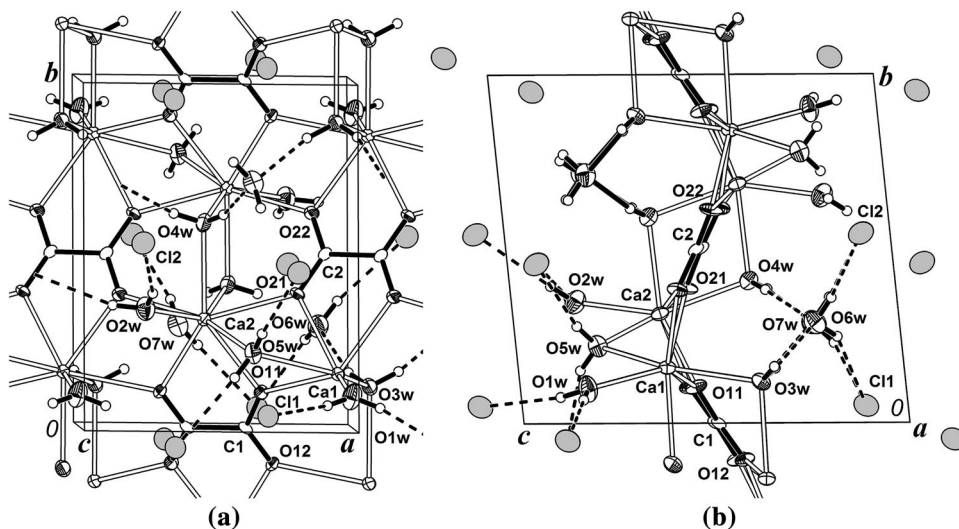

Fig. 2 Crystal packing projections of $Ca_2(C_2O_4)Cl_2 \cdot 7H_2O$; **a** *down* the c-axis; **b** *down* the a-axis

Table 3 Selected bond lengths (Å) and angles (°) for $Ca_2(C_2O_4)Cl_2 \cdot 7H_2O$

Bond lengths (Å)		Angles (°)	
Ca(1)–O(1W)	2.340(3)	O(11)–C(1)–O(12)	126.8(3)
Ca(1)–O(21)	2.441(2)	O(11)–C(1)–C(1)#3	116.5(3)
Ca(1)–O(3W)	2.442(3)	O(12)–C(1)–C(1)#3	116.7(3)
Ca(1)–O(11)	2.467(2)	O(21)–C(2)–O(22)	126.5(3)
Ca(1)–O(3W)#2	2.489(2)	O(21)–C(2)–C(2)#1	116.5(3)
Ca(1)–O(12)#2	2.537(2)	O(22)–C(2)–C(2)#1	117.0(3)
Ca(1)–O(5W)	2.538(3)	C(1)–O(11)–Ca(2)	120.3(2)
Ca(2)–O(2W)	2.370(2)	C(1)–O(11)–Ca(1)	137.7(2)
Ca(2)–O(4W)	2.437(3)	Ca(2)–O(11)–Ca(1)	101.80(8)
Ca(2)–O(11)	2.444(2)	C(1)–O(12)–Ca(2)#3	119.0(2)
Ca(2)–O(12)#3	2.469(2)	C(1)–O(12)–Ca(1)#2	130.9(2)
Ca(2)–O(21)	2.482(2)	Ca(2)#3–O(12)–Ca(1)#2	109.66(7)
Ca(2)–O(4W)#4	2.498(2)	C(2)–O(21)–Ca(1)	119.5(2)
Ca(2)–O(22)#4	2.541(2)	C(2)–O(21)–Ca(2)	138.8(2)
Ca(2)–O(5W)	2.564(3)	Ca(1)–O(21)–Ca(2)	101.45(8)
C(1)–O(11)	1.249(3)	C(2)–O(22)–Ca(1)#1	118.4(2)
C(1)–O(12)	1.254(3)	C(2)–O(22)–Ca(2)#4	131.0(2)
C(1)–C(1)#3	1.555(6)	Ca(1)#1–O(22)–Ca(2)#4	109.82(7)
C(2)–O(21)	1.252(4)	Ca(1)–O(3W)–Ca(1)#2	101.74(9)
C(2)–O(22)	1.257(4)	Ca(2)–O(4W)–Ca(2)#4	103.53(9)
C(2)–C(2)#1	1.549(6)	Ca(1)–O(5W)–Ca(2)	96.67(8)

Symmetry transformations used to generate equivalent atoms: (#1) $-x + 2, -y + 1, -z + 1$; (#2) $-x + 2, -y, -z + 1$; (#3) $-x + 1, -y, -z + 1$; (#4) $-x + 1, -y + 1, -z + 1$

Table 4 Hydrogen bond distances (Å) and angles (°) for $Ca_2(C_2O_4)Cl \cdot 7H_2O$

D-H···A	d(D–H)	d(H···A)	d(D···A)	<(D-H···A)
O(1W)–H(1A)···Cl(1)#5	0.86(1)	2.28(1)	3.128(3)	169(3)
O(1W)–H(1B)···Cl(1)#1	0.85(1)	2.30(1)	3.147(3)	172(3)
O(2W)–H(2A)···Cl(2)#6	0.85(1)	2.44(2)	3.260(3)	161(4)
O(1W)–H(2B)···Cl(2)#5	0.86(1)	2.37(2)	3.189(3)	161(3)
O(3W)–H(3A)···O(6W)	0.85(1)	1.93(2)	2.749(3)	162(3)
O(3W)–H(3B)···O(7W)#2	0.85(1)	1.87(2)	2.704(4)	165(3)
O(4W)–H(4A)···O(7W)	0.860(9)	1.84(2)	2.680(4)	164(4)
O(4W)–H(4B)···O(6W)	0.83(3)	1.96(4)	2.772(4)	165(4)
O(5W)–H(5A)···Cl(2)#4	0.85(1)	2.31(1)	3.144(3)	167(4)
O(5W)–H(5B)···Cl(1)#3	0.85(1)	2.36(2)	3.141(3)	154(4)
O(6W)–H(6A)···Cl(1)	0.86(1)	2.44(2)	3.229(4)	153(3)
O(6W)–H(6B)···Cl(2)#2	0.85(1)	2.44(1)	3.266(3)	164(3)
O(7W)–H(7A)···Cl(1)	0.85(1)	2.25(2)	3.064(3)	159(3)
O(7W)–H(7B)···Cl(2)	0.85(1)	2.24(1)	3.081(3)	167(4)

Symmetry transformations used to generate equivalent atoms: (#1) $-x + 2, -y, -z + 1$; (#2) $x + 1, y, z$; (#3) $-x + 1, -y, -z + 1$; (#4) $-x + 1, -y + 1, -z + 1$; (#5) $x, y, z + 1$; (#6) $-x, -y + 1, -z + 1$

novgorodovaite, the $C_2O_4^{2-}$ anions are planar within experimental accuracy.

As for novgorodovaite, both calcium ions in the higher hydrate are in an eight-fold coordinated environment, but, in this case a pair of water molecules displaces the chlorine ions from the alkaline-earth metal coordination sphere. In fact, the metals are coordinated to four oxalate oxygen (O) and four water oxygen (Ow) atoms through their respective electron pairs (CaO_4Ow_4 polyhedron). Again the crystal packing favors the directional bonding of oxalate, $C_2O_4^{2-}$, ligands to calcium ions through the sp^2 oxygen electron pairs [C–O–Ca angles in the range from 118.4(2)° to 138.8(2)°; average (deviation) = 127(8)°]. This can be appreciated in Fig. 2 (left) which shows that the heptahydrate presents a chain arrangement along a ($a = 7.3928(8)$ Å) closely related to the one reported for novgorodovaite along its crystal b-axis (see Fig. 1, left). The arrangement along the (ab) plane (see Fig. 2, right) resembles a pleated version of the one observed along the ($\bar{1}$ 0 1) plane of novgorodovaite (see Fig. 1, right).

The seven water molecules in $Ca_2(C_2O_4)Cl_2 \cdot 7H_2O$ can be split into two sets. One of these sets (w1–w5) bond to calcium ions [Ca–Ow contact distances in the range from 2.340(3) to 2.564(3) Å] with all their H-atoms involved in OwH···Cl bonds [OwH···Cl distances in the 2.24(1)–2.44(2) Å range and Ow-H···Cl angles in the 159(3)°–172(3)° range] and OwH···Ow bonds with the two water molecules (w6 and w7) of the other set [OwH···Ow distances in the 1.84(2)–1.96(4) Å range and Ow-H···Ow angles in the 162(3)°–165(4)° range]. The members of this latter set are water molecules of crystallization that, besides being acceptor of the above H-bonds from the coordination water molecules also act as donor in OwH···Cl bonds [OwH···Cl distances in the 2.24(1)–2.44(2) Å interval and Ow-H···Cl angles in the 153(3)°–167(4)° range] in a distorted tetrahedral arrangement of H-bonds around the water O6w and O7w oxygen atoms. The H-bonding structure is detailed in Table 4.

The crystal structure comprises $Ca_2(C_2O_4)(H_2O)_5$ slabs parallel to (001) crystal plane, alternating with hydrated chloride layers (see Fig. 2, right). The coordination around Ca(II) ions, saturated by Ca–O(ox) and Ca–Ow contacts, and the choride ions surrounded by water molecules prevent the kind of close ionic Ca^{2+}–Cl^- interactions (Ca–Cl distance of about 2.8 Å) observed in novgorodovaite. In fact, the shorter Ca···Cl distance in the heptahydrate is larger than 4.0 Å.

The two-dimensional nature of the structure in which $Ca_2(C_2O_4)(H_2O)_5$ slabs alternate with weakly bound interlayers containing hydrated chloride, explains why the crystals grow as relatively large thin sheets parallel to (001) plane, which is both an perfect cleavage and also a twin interface plane.

Powder X-ray diffraction

In Figs. 3 and 4, the respective powder X-ray diffraction patterns of synthetic novgorodovaite and $Ca_2(C_2O_4)$ $Cl_2 \cdot 7H_2O$ salt compared with those calculated from the single-crystal XRD data (Yvon et al. 1977). All ten diagnostic lines (see below) for each compound have been indexed on the basis of the corresponding single-crystal diffraction data.

The figures show that the polycrystalline powders have the same crystal structures as their single-crystal counterparts, without significant contribution from other crystalline phases. Differences between experimental and theoretical integrated peak intensities are likely due to preferred orientation in the powder. The orientation effect is particularly notorious for the heptahydrate where the strongest four observed peaks of Fig. 4 are enhanced (00*l*) reflections with *l* = 1–4. This is due to preferred orientation along the crystal reciprocal *c**-axis of the powder pressed onto the sample holder which was employed in the PXRD measurements. The orientation, in turn, is favored by the fact stated above that the heptahydrate grows a very thin crystal plates parallel to (001) plane, Diagnostic powder diffraction peaks are observed at 2θ-values (in degrees) of 16.86, 17.60, 24.12, 30.20, 30.66, 35.57, 38.83, 41.00, 48.91, and 54.52
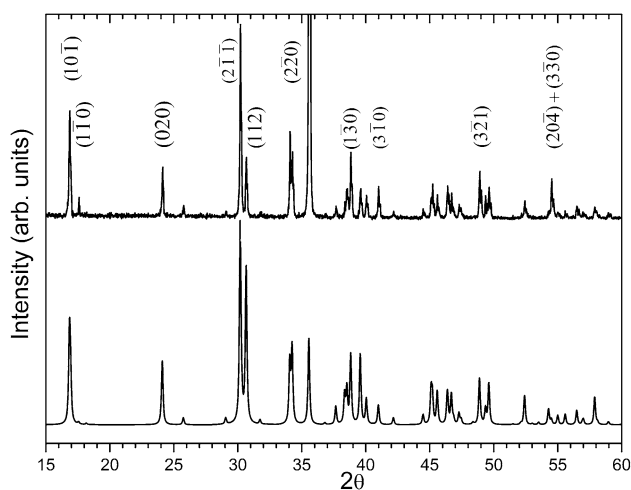

Fig. 4 *Upper trace* experimental PXRD pattern of $Ca_2(C_2O_4)$ $Cl_2 \cdot 7H_2O$. *Lower trace* calculated PXRD pattern of $Ca_2(C_2O_4)$ $Cl_2 \cdot 7H_2O$

for synthetic novgorodovaite and 8.97, 17.99, 19.66, 26.81, 27.10, 29.86, 36.41, 40.12, 43.50, and 46.00 for $Ca_2(C_2O_4)$ $Cl_2 \cdot 7H_2O$, with an estimated error of $\pm 0.03°$.

Vibrational spectra

To extend the characterization of the two investigated compounds, we have measured and briefly analyzed their FTIR and Raman spectra. The comparison of the infrared spectrum of synthetic novgorodovaite with that obtained for a natural sample from Aksai valley, Aktobe region (western Kazakhstan) (Chukanov 2014), shows totally identical spectral patterns, additionally confirming the identity of the synthetic sample.

The FTIR and Raman spectra of synthetic novgorodovaite are shown in Fig. 5 and the proposed assignment is presented in Table 5, and briefly commented as follows:

- An inspection of both spectra immediately shows that there is a lack of coincidences in the position of IR and Raman bands. This fact is in agreement with the structural results, which show the presence of planar $C_2O_4^{2-}$ anions in this crystal lattice, for which the rule of mutual exclusion becomes operative because of the presence of a center of symmetry. In this context, both spectra show close similarities to those of PbC_2O_4, also dominated by the presence of a planar oxalate anion (Mancilla et al. 2009b).
- The characteristic O–H stretching vibrations of the water molecules are seen as a relatively broad but defined IR band centered at 3351 cm^{-1} with some weaker features at the lower and higher energy sides.

Fig. 3 *Upper trace* experimental PXRD pattern of synthetic novgorodovaite collected with CuKα radiation. *Lower trace* PXRD pattern calculated from the solid-state molecular structure of synthetic novgorodovaite
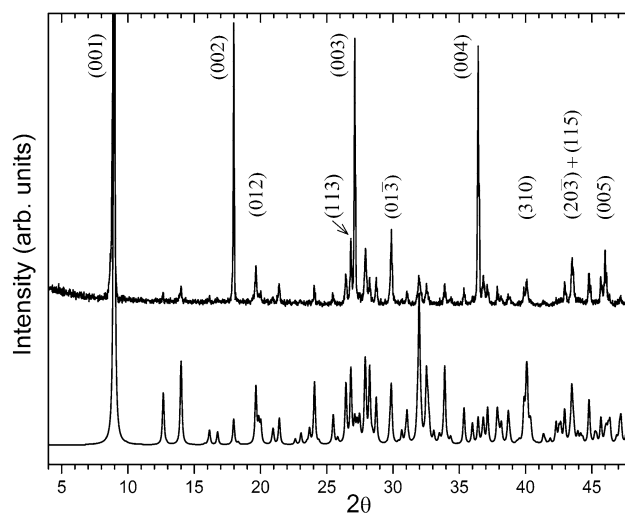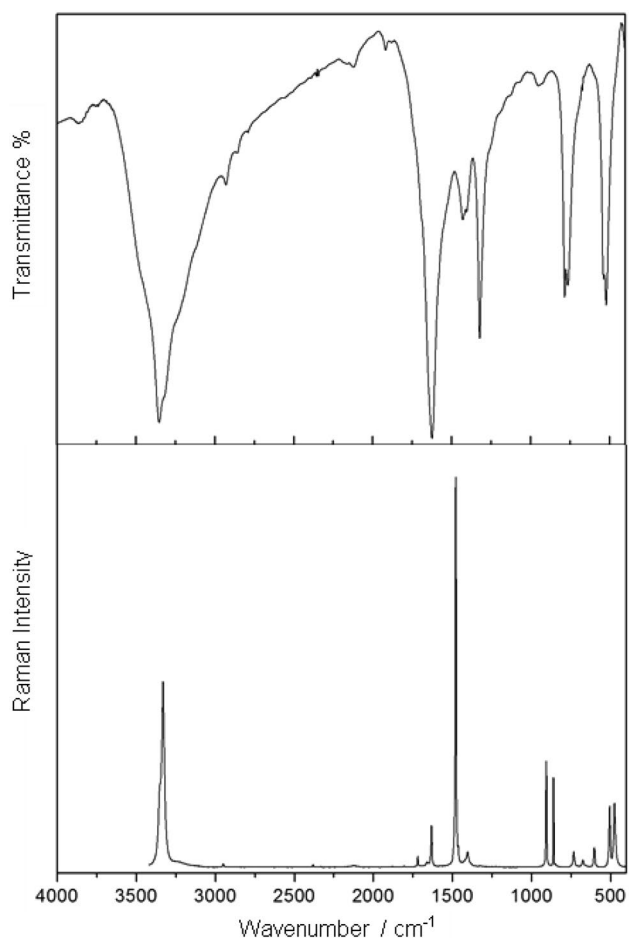
Fig. 5 FTIR (*above*) and FT-Raman spectra (*below*) of synthetic novgorodovaite, $Ca_2(C_2O_4)Cl_2 \cdot 2H_2O$

Table 5 Assignment of the vibrational spectra of synthetic novgorodovaite, $Ca_2(C_2O_4)Cl_2 \cdot 2H_2O$ (band positions in cm^{-1})

Infrared	Raman	Assignment
3580 sh, 3551 vs		ν(OH) water
3318 sh, 3240 sh	3350 sh, 3330 s	ν(OH) water
1690 sh, 1622 vs		ν_{as}(COO)
	1717 vw	Overtone, cf. text
	1630 w, 1477 vs	ν_s(COO)
1426 m		(?)
	1402 vw	Combination, cf. text
1320 s		ν_{as}(COO)
948 w, 928 sh		$\rho(H_2O)$
	904 s, 859 s	ν(C–C)
782 s, 762 s		δ_{as}(OCO)
	730 w, 673 vw, 600 w	$\rho(H_2O)$
536 sh, 519 s		ρ(OCO)
	503 s, 472 s	δ_s(OCO)

vs very strong, *s* strong, *m* medium, *w* weak, *vw* very weak, *sh* shoulder

In the Raman spectrum, a unique and well-defined band is observed at 3330 cm^{-1} with a weak shoulder at higher energies. The positions of these vibrations suggest that the H-bonds are of moderate strength (Siebert 1966). The bending modes of the water molecules are surely overlapped by the strong carboxylate IR band located at about 1620 cm^{-1}. Some water librational modes were tentatively assigned in both the IR and Raman spectra by comparison with the spectral data of $CaC_2O_4 \cdot H_2O$ (Petrov and Soptrajanov 1975; Conti et al. 2014), $SrC_2O_4 \cdot H_2O$ and $SrC_2O_4 \cdot 2H_2O$ (D'Antonio et al. 2015) as well as $BaC_2O_4 \cdot 0.5H_2O$ (Torres et al. 2016). Notwithstanding, it is difficult to decide which librational mode (rocking, wagging or twisting) is effectively involved in each of the observed spectral features.

- For the motions of the carboxylate groups in a planar C_2O_4 anion, one expects two IR-active antisymmetric stretching vibrations and two Raman-active symmetric stretching vibrations (Hind et al. 1998; Mancilla et al. 2009b). These expectations are clearly fulfilled in the present case, although the higher-frequency ν_{as}-mode shows an additional shoulder at 1690 cm^{-1} probably originated in correlation field effects.

- One of the components of the symmetric COO-stretching mode is the strongest band observed in the Raman spectrum, whereas the other component, located at somewhat higher energies, is unusually weak. The corresponding antisymmetric motion is the strongest IR band. The characteristic ν(C–C) stretching is only observed, as expected (Mancilla et al. 2009b), in the Raman spectrum. Its splitting is surely also a consequence of correlation field effects.

- The assignment of the two δ(OCO) modes was made on the basis of previous results obtained with PbC_2O_4 (Mancilla et al. 2009b) and with the alkali-metal oxalates (Shippey 1980; Clark and Firth 2002).

- Two very weak Raman features could be assigned to overtone and combination bands (1717 cm^{-1} vw = 2 × 859 cm^{-1}; 1402 cm^{-1} vw = 904 + 503 cm^{-1}). Similar bands are also observed in the case of PbC_2O_4 and the alkaline-metal oxalates. Interestingly, a medium intensity IR band at 1426 cm^{-1}, also observed in the case of the natural novgorodovaite (Chukanov 2014) and in PbC_2O_4 (Mancilla et al. 2009b), could not be assigned confidently and it is, eventually, a combination mode of a fundamental with a low lying external (lattice) vibration.

The vibrational spectra of $Ca_2(C_2O_4)Cl_2 \cdot 7H_2O$ are shown in Fig. 6 and the proposed assignment, presented in Table 6, is briefly discussed as follows:

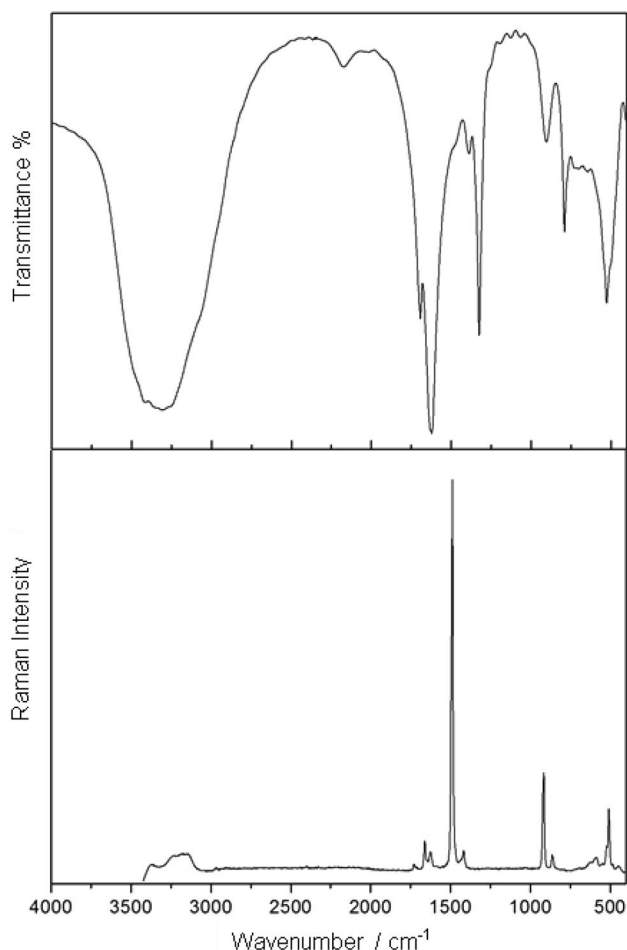**Fig. 6** FTIR (*above*) and FT-Raman spectra (*below*) of $Ca_2(C_2O_4)$ $Cl_2 \cdot 7H_2O$

Table 6 Assignment of the vibrational spectra of $Ca_2(C_2O_4)$ $Cl_2 \cdot 7H_2O$ (band positions in cm^{-1})

Infrared	Raman	Assignment
3305 vs	3230 w, 3145 w	$\nu(OH)$ water
1691 w, 1620 vs		$\nu_{as}(COO)$
	1725 vw	Overtone, cf. text
	1659 w,1624 vw, 1477 vs	$\nu_s(COO)$
	1416 vw	Combination, cf. text
1385 w, 1323 s		$\nu_{as}(COO)$
903 s		$\nu(C–C)$
	915 s, 862 w	$\nu(C–C)$
789 s		$\delta_{as}(OCO)$
700 vw, 645 vw		$\rho(H_2O)$
	584 vw	$\rho(H_2O)$
525 vs, 497 sh		$\rho(OCO)$
	506 m, 448 vw	$\delta_s(OCO)$

vs very strong, *s* strong, *m* medium, *w* weak, *vw* very weak, *sh* shoulder

spectrum, accompanied by some weak features at the higher energy side.

- Deformational modes of the oxalate groups and the characteristic $\nu(C–C)$ vibration are found almost at the same energies as in $Ca_2(C_2O_4)Cl_2 \cdot 2H_2O$.
- Also in this case, one overtone and one combination mode could be identified. The very weak Raman band at 1725 cm^{-1} is probably the first overtone of the $\nu(C–C)$ component at 862 cm^{-1}, whereas the other very weak Raman band at 1416 cm^{-1} may be a combination between the second $\nu(C–C)$ component and the 506 cm^{-1} $\delta_s(OCO)$ component.

Conclusions

From the performed study, we can draw the following main conclusions:

1. We prepared synthetic novgorodovaite, $Ca_2(C_2O_4)$ $Cl_2 \cdot 2H_2O$, and refined the reported crystal structure of the natural solid against our synthetic single-crystal X-ray diffraction data to prove that the solids are coincident. This is further confirmed by the comparison of their respective IR absorption spectra.
2. Seventy years after the report of its preparation, crystal morphology, and some crystal *d*-spacing, we present here the detailed solid-state structure of the heptahydrate analog of novgorodovaite, namely $Ca_2(C_2O_4)$ $Cl_2 \cdot 7H_2O$, which crystals grow as triclinic ($P\bar{1}$) twins. Confirming and fully specifying the early report, the crystals of this salt grow as very thin lamellae parallel

- The (O–H) stretching vibrations of the water molecules generate a very strong and broad IR band centered at 3305 cm^{-1} whereas in the Raman spectrum only two very weak features (3230 and 3145 cm^{-1}) can be observed. The frequencies of these bands, lower than that for novgorodovaite, suggest that the H-bonds are moderate to high in strength (Siebert 1966). Again, the $\delta(H_2O)$ modes are overlapped by the strong oxalate vibration at around 1600 cm^{-1}. Two water librational modes were also assigned, using the same criteria as mentioned above.
- The strongest IR band, found at 1620 cm^{-1} and assigned to the antisymmetric oxalate stretching vibration, appears clearly split in this case, whereas for synthetic novgorodovaite only a shoulder can be seen at the higher energy side. Also the second $\nu_{as}(COO)$ vibrations appears clearly split. Also in this case, these splittings may be originated in correlation field effects. The corresponding symmetric stretching mode is, also in this case, the strongest line in the Raman

to (001) plane which is both a perfect cleavage and a twin interface plane. Probably, early attempts of crystal structure determination and refinement were hampered by the unavoidable tendency of the heptahydrate analog to grow as twinned crystals, the difficulties in collecting diffraction data from multiple single-crystal domains employing photographic or scintillation-counter methods, and also the lack of now routine procedures to disentangle the diffraction intensities in terms of two or more contributing single-crystal domains that afford a smooth structure refinement (Parsons 2003).

3. Unlike novgorodovaite, the water molecules in the higher hydrated salt prevent direct Ca–Cl bonding, while preserving polymeric structural units defined by Ca–C_2O_4 bonding. In fact, in both salts the crystal packing favors the directional bonding of oxalate ligands to calcium ions through the oxygen sp^2 electron pairs, a bonding pattern also observed in other calcium oxalate salts.

4. The crystal packing of the triclinic heptahydrate along the (001) plane resembles a pleated version of the one observed along the ($\bar{1}$ 0 1) plane of monoclinic novgorodovaite (with chlorine replaced by water molecules) but differs radically in the other direction. In fact, the $Ca_2(C_2O_4)Cl_2 \cdot 7H_2O$ structure is arranged as $Ca_2(C_2O_4)(H_2O)_5$ slabs parallel to (001) crystal plane with hydrated chloride ions in the interlayer spaces, which accounts for the above-mentioned peculiar physical properties.

5. The analysis of the vibrational (infrared and Raman) spectra of both hydrates, and their comparison with spectroscopic data of other oxalato complexes, clearly shows that they are dominated by the vibrations of the planar $C_2O_4^{2-}$ groups and water molecules.

References

Baran EJ (2016) Natural iron oxalates and their analogous synthetic counterparts: a review. Chem Erde-Geochem 76:449–460

Baran EJ, Monje PV (2008) Oxalate biominerals. In: Sigel A, Sigel H, Sigel RKO (eds) Metal ions in life sciences, vol 4. Biomineralization, from nature to applications. Wiley, Chichester, pp 219–254

Chukanov NV (2014) Infrared spectra of mineral species, vol 1. Springer, Dordrecht

Chukanov NV, Belakovskii DI, Rastsvetaeva RK, Karimova OV, Zadov AE (2001) Novgorodovaite, $Ca_2(C_2O_4)Cl_2 \times 2H_2O$, a new mineral. Zapiski VMO 130(4):32–35 **(in Russian)**

Clark RJH, Firth S (2002) Raman, infrared and force field studies of $K_2^{12}C_2O_4 \cdot H_2O$ and $K_2^{13}C_2O_4 \cdot H_2O$ in the solid state and in aqueous solution, and of $(NH_4)_2^{12}C_2O_4 \cdot H_2O$ and $(NH_4)_2^{13}C_2O_4 \cdot H_2O$ in the solid state. Spectrochim Acta 58A:1731–1746

Conti C, Casati M, Colombo Ch, Realini M, Brambilla L, Zerbi G (2014) Phase transformation of calcium oxalate dihydrate-monohydrate: effects of relative humidity and new spectroscopic data. Spectrochim Acta 128A:413–419

Cotton FA, Wilkinson G, Murillo CA, Bochmann M (1999) Advanced inorganic chemistry, 6th edn. Wiley, New York, pp 484–488

CrysAlisPro (2014) Oxford Diffraction Ltd., Version 1.171.37.31 (release 14-01- 2014 CrysAlis171.NET)

D'Antonio MC, Palacios D, Coggiola L, Baran EJ (2007) Vibrational and electronic spectra of synthetic moolooite. Spectrochim Acta 68A:424–426

D'Antonio MC, Wladimirsky A, Palacios D, Coggiola L, González-Baró AC, Baran EJ, Mercader RC (2009) Spectroscopic investigation of the iron(II) and iron(III) oxalates. J Braz Chem Soc 20:445–450

D'Antonio MC, Mancilla N, Wladimirsky A, Palacios D, González-Baró AC, Baran EJ (2010) Vibrational spectra of magnesium oxalates. Vibrat Spectr 53:218–221

D'Antonio MC, Torres MM, Palacios D, González-Baró AC, Baran EJ (2015) Vibrational spectra of the two hydrate of strontium oxalate. Spectrochim Acta 137A:486–489

Deganello S, Piro OE (1981) The crystal structure of calcium oxalate monohydrate (whewellite). Neues Jahrb Miner Monatsh 1981:81–88

Echigo T, Kimata M (2010) Crystal chemistry and genesis of organic minerals, a review of oxalate and polycyclic aromatic hydrocarbon minerals. Can Miner 48:1329–1358

Farrugia LJ (1997) ORTEP-3 for windows-a version of ORTEP-III with a graphical user interface (GUI). J Appl Crystallogr 30:565

Franceschi VR, Nakata PA (2005) Calcium oxalate in plants: formation and function. Ann Rev Plant Physiol 56:41–71

Hind AR, Bhargava SK, van Bronswijk W, Grocott SC, Eyer SL (1998) On the aqueous vibrational spectra of alkali metal oxalates. Appl Spectr 52:683–691

Jones FT, White LM (1946) The composition, optical and crystallographic properties of two calcium oxalate–chloride double salts. J Am Chem Soc 68:1339–1342

Mancilla N, Caliva V, D'Antonio MC, González-Baró AC, Baran EJ (2009a) Vibrational spectroscopic investigation of the hydrates of manganese(II) oxalates. J Raman Spectr 40:915–920

Mancilla N, D'Antonio MC, González-Baró AC, Baran EJ (2009b) Vibrational spectra of lead(II) oxalate. J Raman Spectr 40:2050–2052

Martell AE, Smith RM (eds) (1977) Critical stability constants, vol 3. Plenum Press, New York, pp 92–96

Mills SJ, Christy AG (2006) The great barrier reef expedition 1928–1929: the crystal structure of and occurrence of weddellite, ideally CaC2O4·2.5H2O, from the Low Isles,Queensland. Miner Mag 80:399–406

Nakata PA (2003) Advances in our understanding of calcium oxalate crystal formation and function in plants. Plant Sci 164:901–909

Parsons S (2003) Introduction to twinning. Acta Crystallogr D59:1995–2003 **and references therein**

Petrov I, Soptrajanov B (1975) Infrared spectrum of whewellite. Spectrochim Acta 31A:309–316

Piro OE, Echeverría GA, González-Baró AC, Baran EJ (2016) Crystal and molecular structure and spectroscopic behavior of isotypic synthetic analogs of the oxalate minerals stepanovite and zhemchuzhnikovite. Phys Chem Miner 43:287–300

Rastsvetaeva RK, Chukanov NV, Nekrasov YuV (2001) Crystal structure of novgorodovaite $Ca_2(C_2O_4)Cl_2 \cdot 2H_2O$. Doklady Chem 381:329–331

Serezhkin VN, Artem'eva MY, Serezhkina LB, Mikhailov YN (2005) Crystal chemical role of oxalate ions. Russ J Inorg Chem 50:1019–1030

Sheldrick GM (2008) A short history of SHELX. Acta Crystallogr A 64:112–122

Shippey TA (1980) Vibrational studies of anhydrous lithium, sodium and potassium oxalates. J Mol Struct 67:223–233

Siebert H (1966) Anwendungen der Schwingunsspektrskopie in der Anorganischen Chemie. Springer, Berlin

Strunz H, Nickel EH (2001) Strunz Mineralogical Tables. E. Schweitzbart'sche Verlagsbuchhandlung, Stuttgart, pp 717–721

Tazzoli V, Domeneghetti C (1980) The crystal structures of whewellite and weddellite: re-examination and comparison. Amer Mineral 65:327–334

Torres MM, Palacios D, D'Antonio MC, González-Baró AC, Baran EJ (2016) Vibrational spectra of barium oxalate hemihydrate. Spectr Lett 49:238–240

Webb MA (1999) Cell-mediated crystallization of calcium oxalate in plants. Plant Cell 11:751–761

Yvon K, Jeitschko W, Parthé E (1977) LAZY PULVERIX, a computer program for calculating X-ray and neutron diffraction powder patterns. J Appl Cryst 10:73–74

Zobel D, Luger P, Dreissig W, Koritsanszky T (1992) Charge density studies on small organic molecules around 20 K: oxalic acid dihydrate at 15 K and acetamide at 23 K. Acta Crystallogr B 48:837–848